MP 4.7 Tunable, Switchable, High-*Q* VHF Microelectromechanical Bandpass Filters

Clark T.-C. Nguyen, Ark-Chew Wong, Hao Ding

University of Michigan, Ann Arbor, MI

Recent atttempts to reduce the cost and size of wireless transceivers feature higher levels of transistor integration in alternative architectures to reduce the need for the off-chip, high-*Q* passives used in present-day super-heterodyne transceivers. Unfortunately, removal of off-chip passives often comes at the cost of increased power consumption in circuits preceding and including the analog-to-digital converter (ADC), which must have higher dynamic ranges to avoid desensitization caused by larger adjacent channel interferers. A selectivity (*Q*) versus power trade-off is seen here.

This device makes possible a paradigm-shifting transceiver architecture that, rather than eliminate high-*Q* passive components, attempts to maximize their role with the intention of harnessing the above *Q* versus power trade-off. One example of this architecture, shown in Figure 4.7.1, uses an extremely high-*Q* RF filter to select the desired channel up at RF, rejecting not only out-of-band interferers, but also adjacent channel interferers. By eliminating adjacent channel interferers, significant power savings are obtained in the low-noise amplifiers (LNAs) and local oscillators. In particular, without adjacent channel interferers to create desensitizing intermodulation components, linearity of the first LNA can now be greatly relaxed, allowing substantial power savings. In addition, the phase noise requirement in the receive path local oscillator can also be relaxed with resulting power savings, since superimposed phase noise tails from interferers are less of an issue. If channel-select filters with both sufficiently high *Q* and power handling capability are available and placed just before the transmitting antenna, similar power savings are possible for the transmit local oscillator and power amplifier, as well.

Due to *Q* limitations, conventional IC technologies cannot attain sufficient selectivity to realize the filters needed in this architecture. In addition, although some off-chip passive filters attain the needed selectivity in some frequency ranges, these lack the required tuning range, so are also inadequate for this application. This paper reports on an IC-compatible passive filter that achieves the needed selectivity by processing signals in the mechanical (rather than electrical) domain using a network of high *Q* (~10,000 under vacuum, c.f., Figure 4.7.2) mechanically vibrating beams, and that is both switchable and tunable via applied control voltages. Figure 4.7.3 presents the scanning electron micrograph (SEM) of a two-resonator (i.e., two-pole) VHF version of this micromechanical filter achieved using a polysilicon surface-micromachining technology. As shown, this device is comprised of two identical, clamped-clamped beam resonators coupled mechanically to one another by a flexural mode beam, and interfaced to surrounding electronics by capacitive transducers realized via polysilicon strips underlying each resonator at various locations.

Figure 4.7.4 presents a perspective-view schematic of the filter in a typical bias and excitation scheme. As shown, under normal operation a dc-bias voltage V_P is applied to the conductive filter structure, while an ac excitation v_i is applied to the input electrode. This voltage combination generates a force component proportional to the product $V_P v_i$ that drives the mechanical system into *x*-directed resonance when the frequency of v_i falls within the filter passband. Motion of the output resonator then creates a dc-biased, time-varying capacitor at the output port $C_o(t)$, that in turn sources an output current given by $i_x = V_P(\delta C_o / \delta t)$. In effect, electrical input signals are converted to mechanical signals, processed in the mechanical domain, and re-converted to electrical signals at the output, ready for further processing by subsequent transceiver stages. Because both the input force and output currents are directly proportional to V_P, this device can be switched in and out by application and removal, respectively, of V_P. Note that this switching function can be further extended to implement a mixer capability.

The center frequency of this filter is set by the frequency f_o of the constituent resonators, while its bandwidth is determined by the ratio of coupling beam (k_{s12}) and resonator (k_r) stiffnesses. As such, the design of this filter involves two main steps: (1) design of mechanical resonators with resonance frequencies equal to f_o and with reasonable stiffnesses k_r; and (2) design of the coupling spring with an appropriate stiffness and with dimensions corresponding to a quarter-wavelength of the filter center frequency. As shown in Figure 4.7.4, an equivalent electrical circuit comprised of series LCR tanks, mechanical and electromechanical impedance transformers, and a capacitive *T*-network to model the transmission line behavior of the coupler, can be obtained via electromechanical analogy, and is often useful as both a design aide and a system verification tool.

The frequency f_o of each resonator, and hence, of the filter, depends on not only geometry and material properties, but also on the bias voltages applied across the transducer capacitors. This results primarily from displacement-to-capacitance nonlinearity that gives rise to voltage-dependent electrical stiffnesses k_e that subtract from the mechanical stiffness k_m of the resonator. As a result, assuming V_P is held constant, the passband shape and center freqency of the filter can be tuned via adjustment of the $V_{i\Delta f}$ voltages shown in Figure 4.7.4. The amount of tuning available can be on the order of 1.25%, as shown in Figure 4.7.5, which plots frequency versus V_P for a 32MHz micromechanical resonator.

Figure 4.7.7 presents the measured transmission spectrum for the filter of Figure 4.7.3. As shown, a 34.5MHz VHF center frequency is realized with 1.3% bandwidth and 2dB associated insertion loss. Even better performance, rivaling that of many off-chip, high-*Q* filters, is attained at HF with 0.2% bandwidths (Figure 4.7.6) [1]. Although the demonstrated VHF range of both Figures 4.7.2 and 4.2.7 is already applicable to radio systems with RF frequencies in the 30-88MHz range, frequency extension research continues, and gigahertz frequencies are not unreasonable.

One of the major advantages of micromechanical filters is that, because of their tiny size and ideally zero dc power dissipation, many (perhaps hundreds or thousands) can be fabricated onto a smaller area than occupied by a single macroscopic filter of today. For wideband applications, rather than use a single tunable filter to select one of several channels over a large frequency range, a massively parallel bank of switchable, tunable micromechanical filters can be utilized, in which desired frequency bands can be switched/tuned in, as needed. By further exploiting the switching flexibility of such a system, resilient frequency-hopping spread spectrum transceiver architectures can be envisioned.

Acknowledgements:
This work was supported under DARPA Cooperative Agreement No. F30602-97-2-010, with some portions funded by the National Science Foundation (NSF) and an Army Research Office (ARO) MURI.

Reference:
[1] F. D. Bannon III, J. R. Clark, and C. T.-C. Nguyen, "High Frequency Microelectromechanical IF Filters," *Technical Digest*, IEEE International Electron Devices Meeting, San Francisco, California, December 8-11, 1996, pp. 773-776.

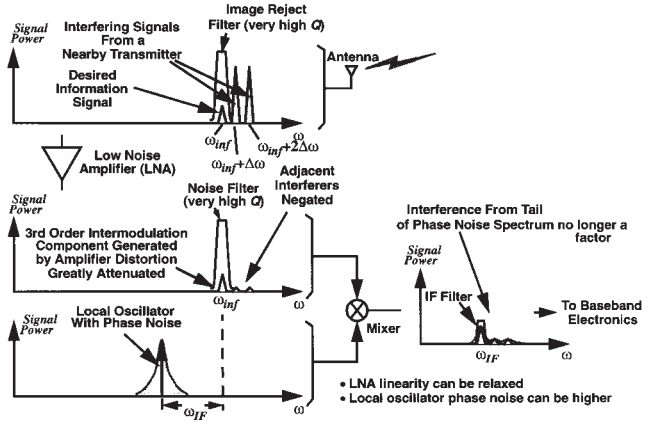

Figure 4.7.1: **RF channel-select receiver architecture and signal flow.**

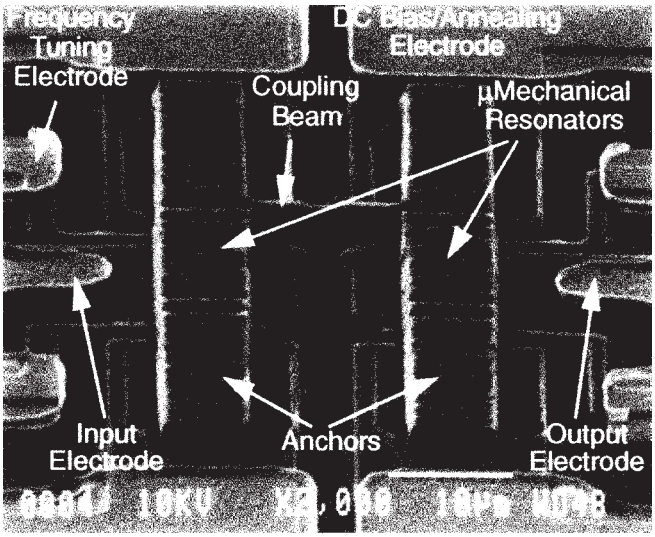

Figure 4.7.3: **SEM of VHF (f_o=34.5MHz) micromechanical filter.**

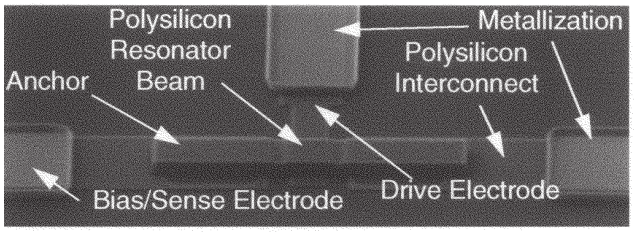

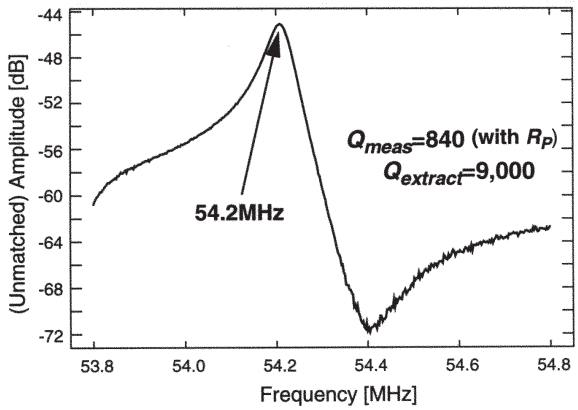

Figure 4.7.2: **SEM and measured frequency characteristic of VHF clamped-clamped beam micromechanical resonator.**

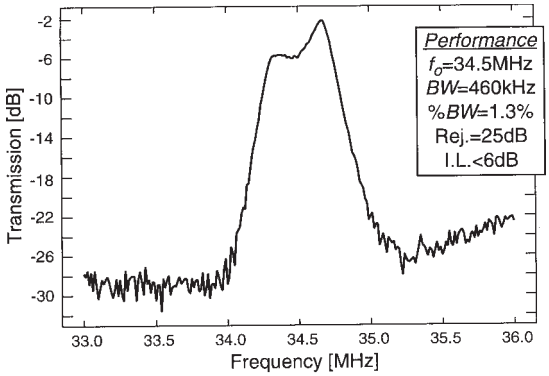

Figure 4.7.5: **Measured transmission spectrum for filter of Figure 4.7.3.**

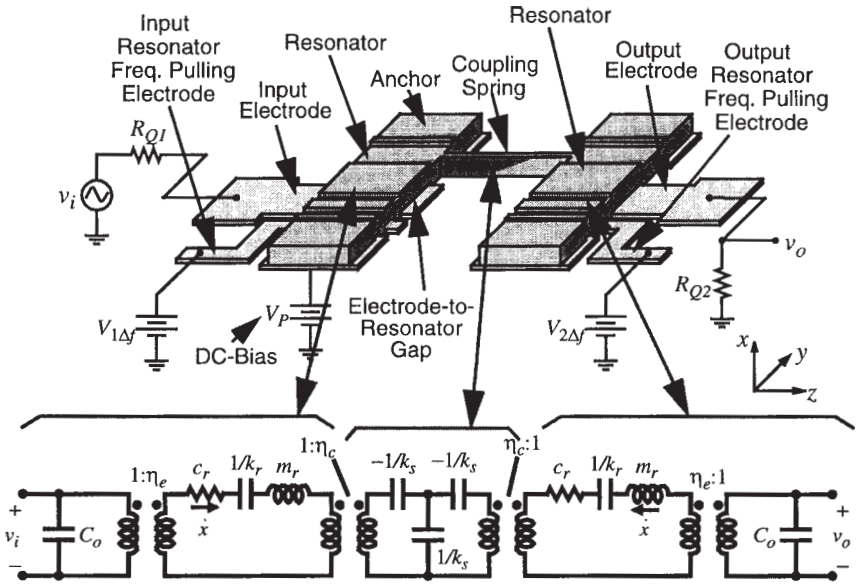

Figure 4.7.4: **Schematic and equivalent circuit for switchable, frequency-tunable micromechanical filter.**

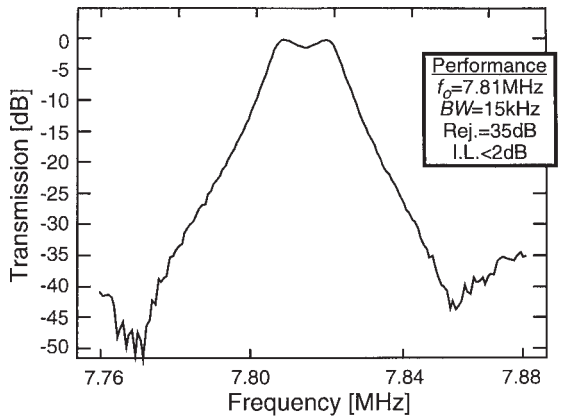

Figure 4.7.6: Measured transmission spectrum for HF (f_o=7.81MHz) micromechanical filter.

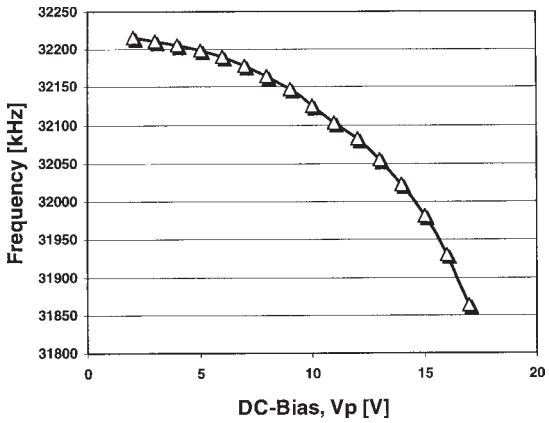

Figure 4.7.7: Measured frequency vs. DC-bias VP for 32MHz resonator.

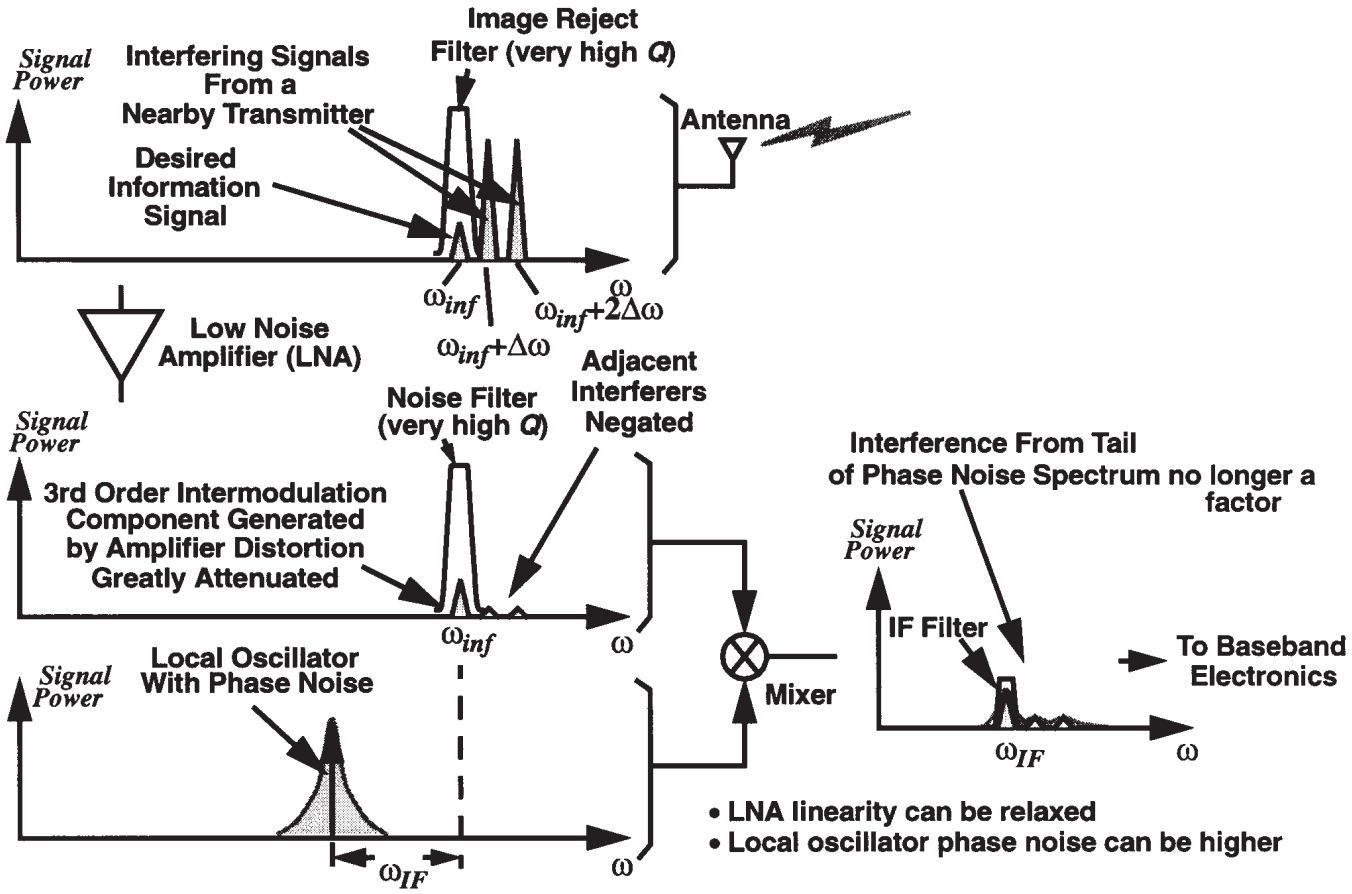

Figure 4.7.1: RF channel-select receiver architecture and signal flow.

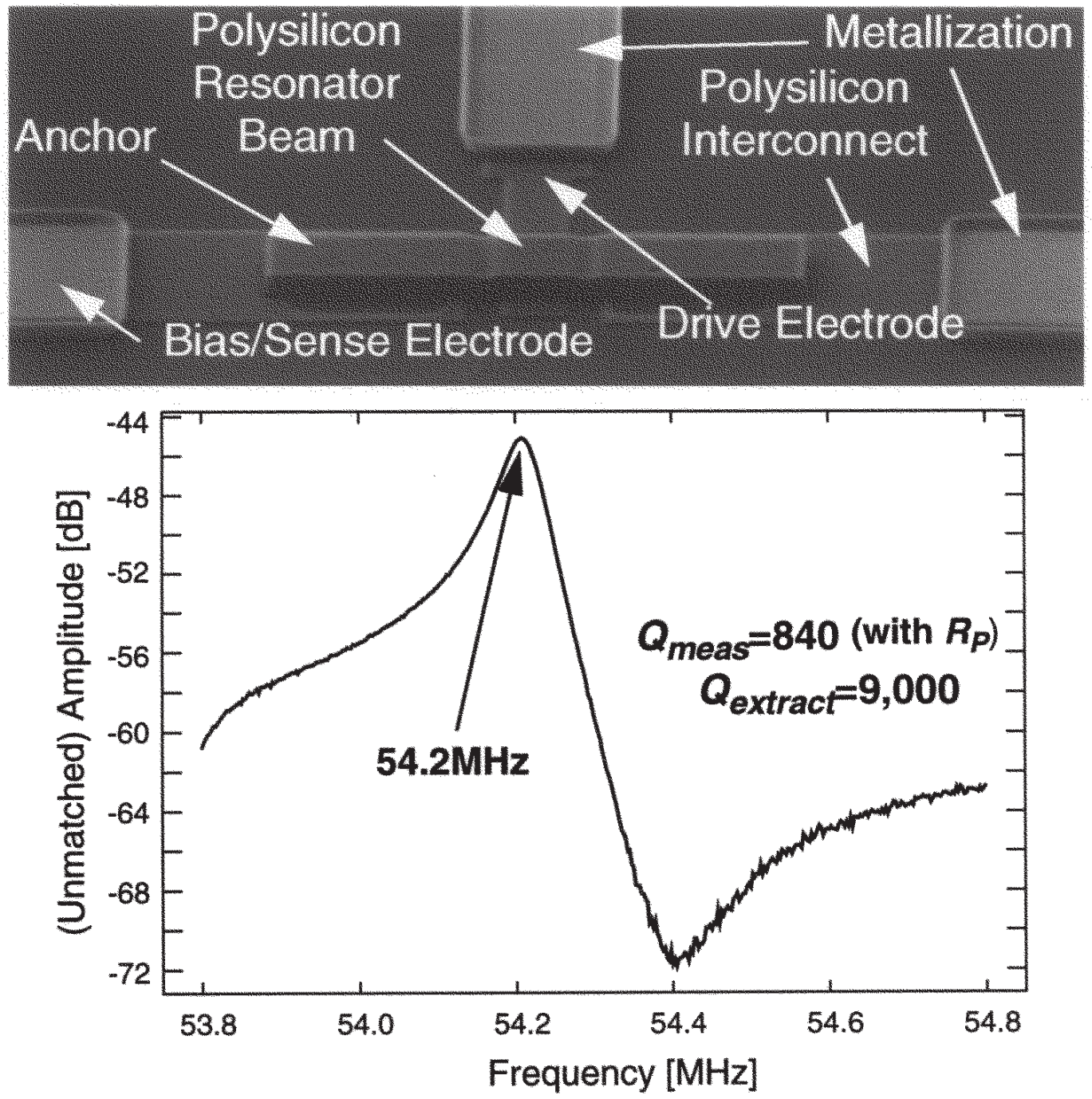

Figure 4.7.2: SEM and measured frequency characteristic of VHF clamped-clamped beam micromechanical resonator.

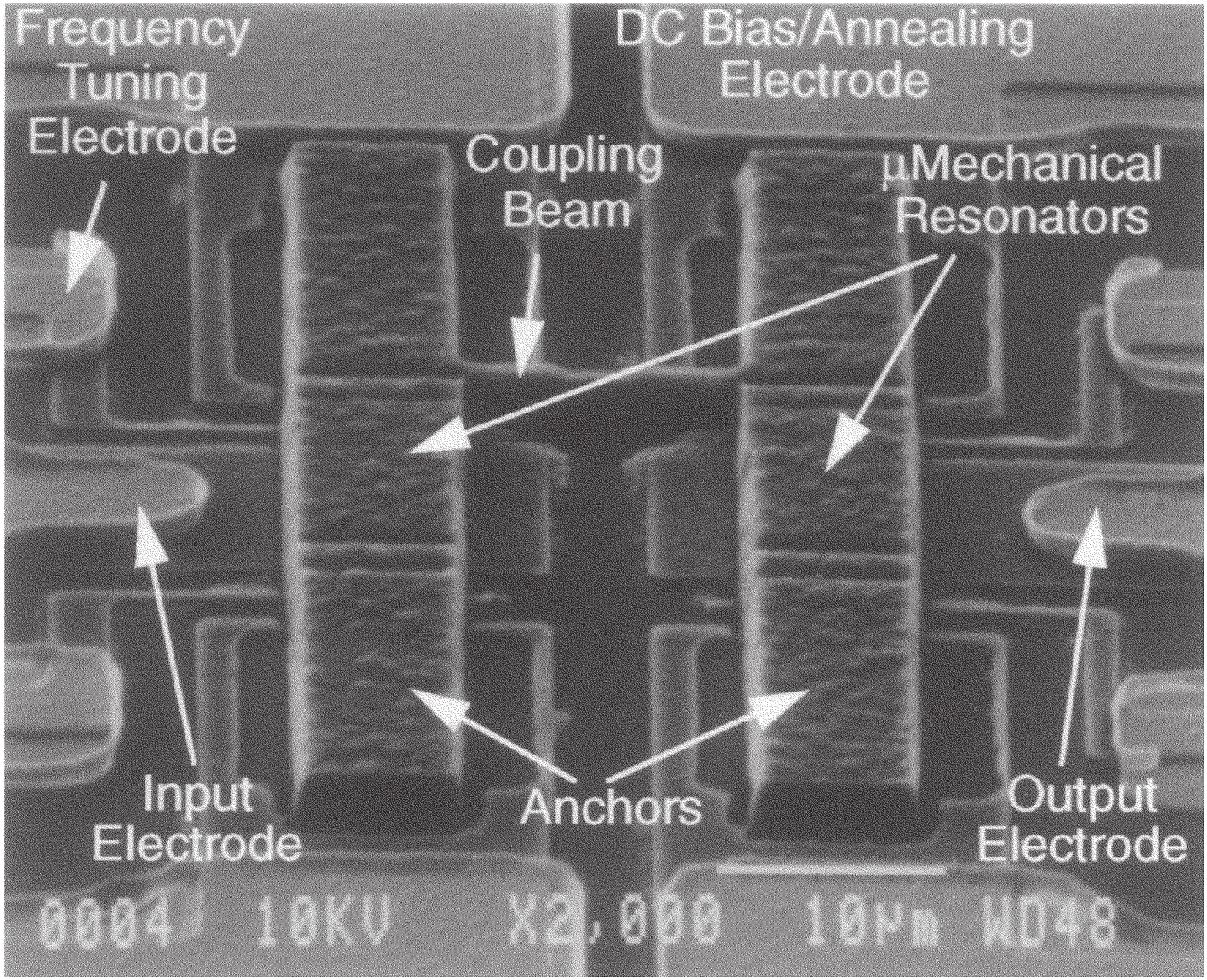

Figure 4.7.3: SEM of VHF (f_o=34.5MHz) micromechanical filter.

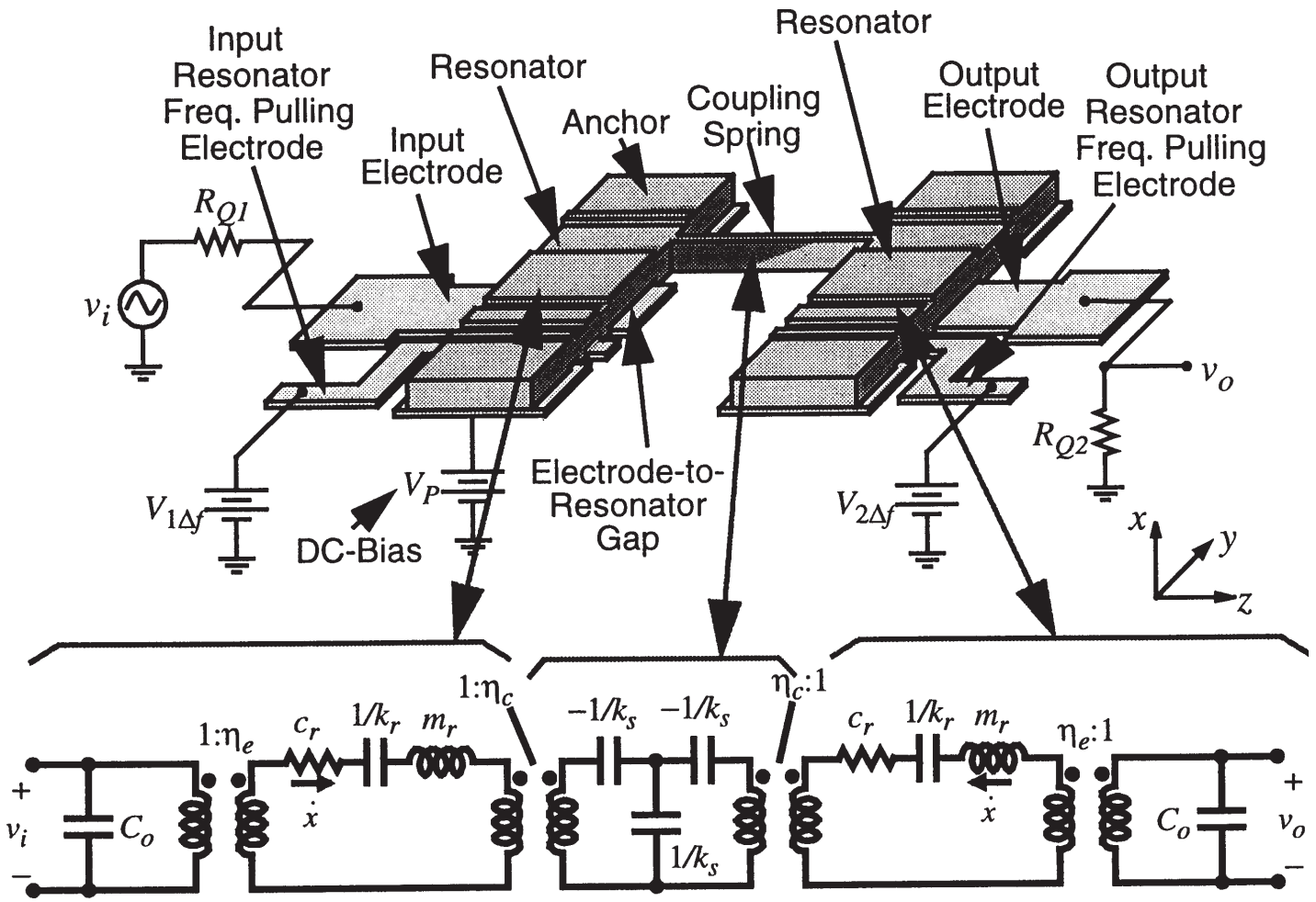

Figure 4.7.4: Schematic and equivalent circuit for switchable, frequency-tunable micromechanical filter.

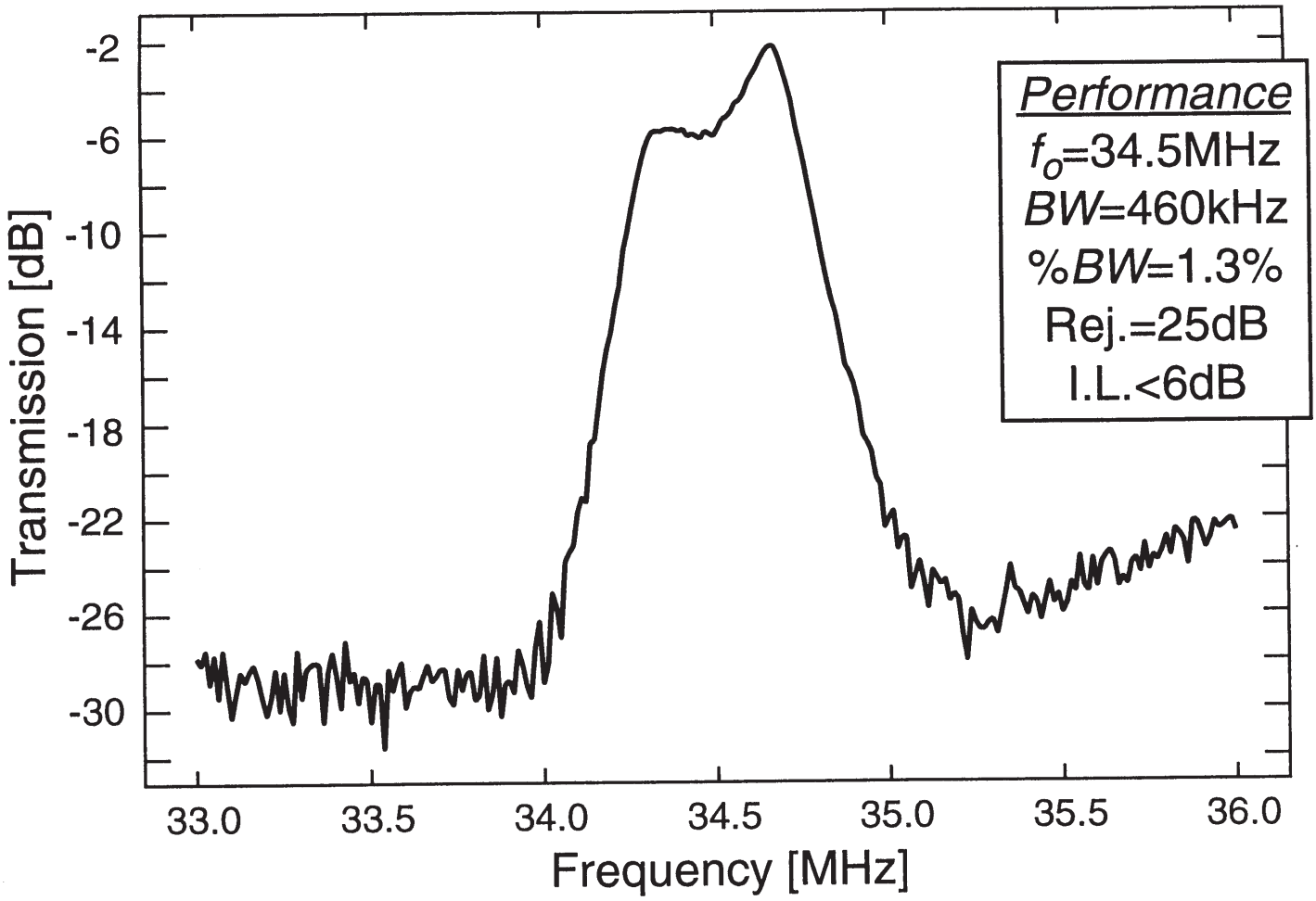

Figure 4.7.5: Measured transmission spectrum for filter of Figure 4.7.3.

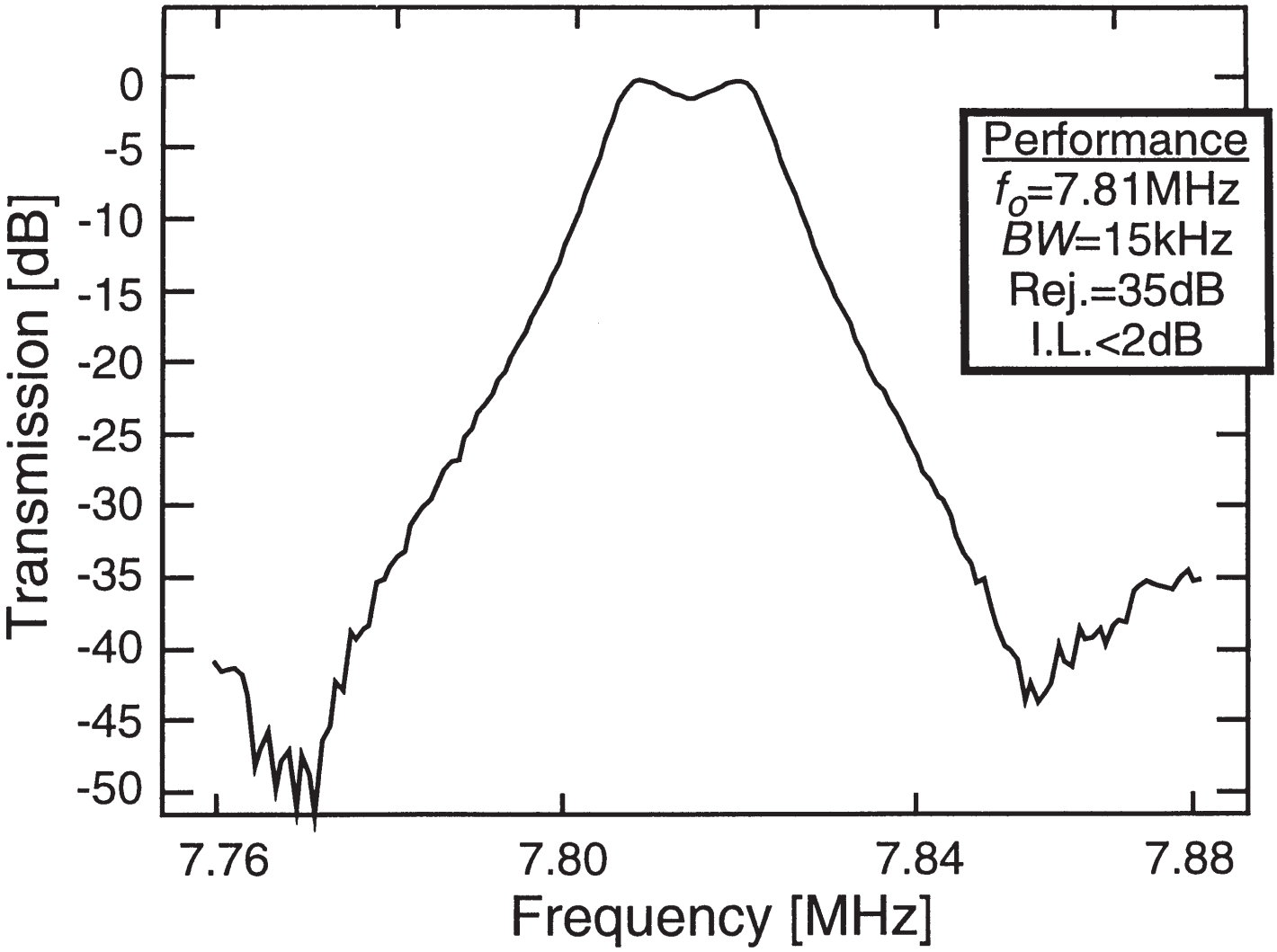

Figure 4.7.6: Measured transmission spectrum for HF (f_o=7.81MHz) micromechanical filter.

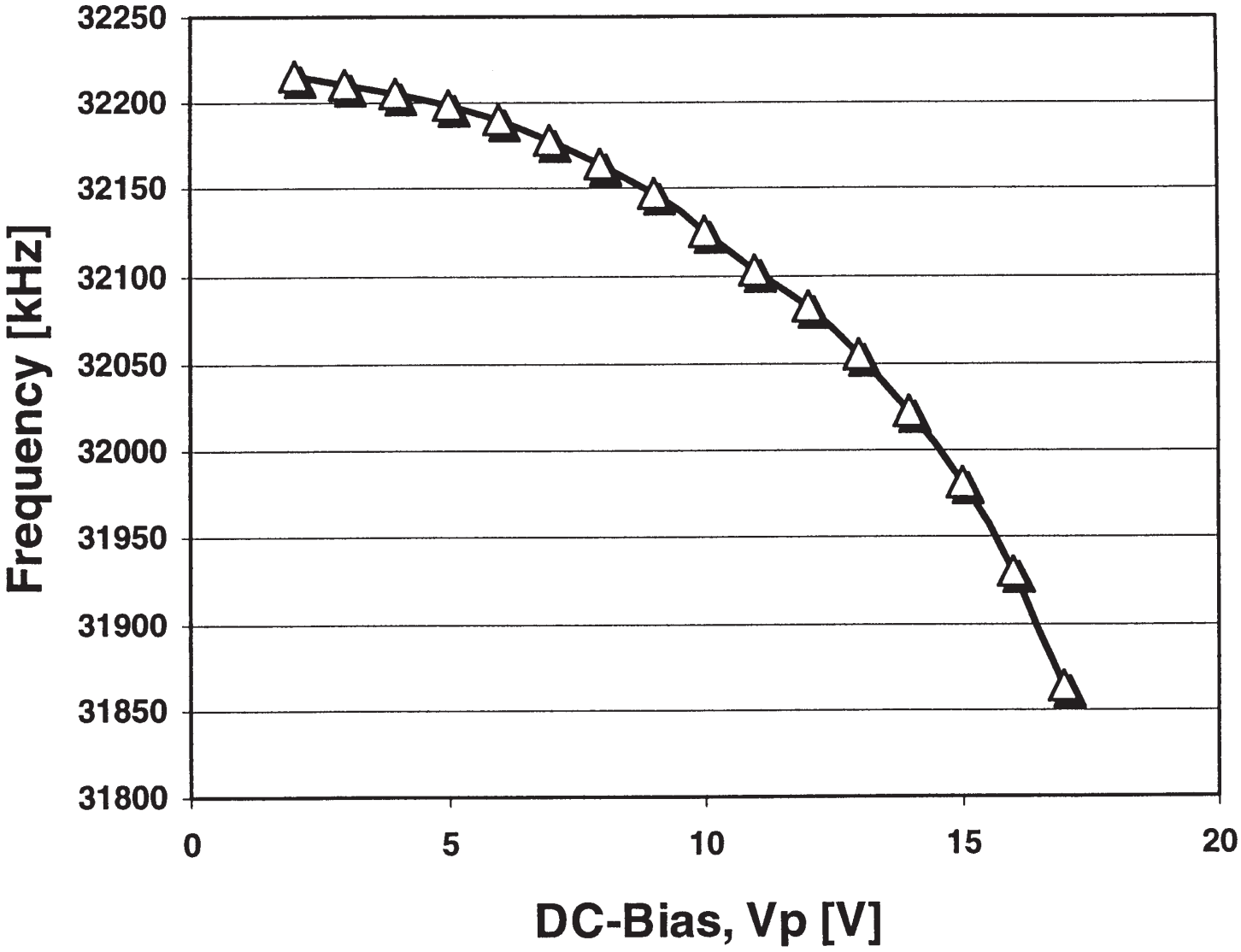

Figure 4.7.7: Measured frequency vs. DC-bias VP for 32MHz resonator.

